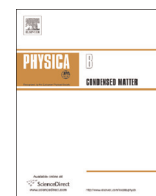




ELSEVIER

Contents lists available at ScienceDirect

Physica B

journal homepage: www.elsevier.com/locate/physb

Suppression of dense Kondo state in CeB₆ under pressure

N. Foroozani^a, J. Lim^a, G. Fabbris^{a,b}, P.F.S. Rosa^c, Z. Fisk^c, J.S. Schilling^{a,*}

^a Department of Physics, Washington University, CB 1105, One Brookings Dr, St. Louis, MO 63130, USA

^b Advanced Photon Source, Argonne National Laboratory, Argonne, IL 60439, USA

^c Department of Physics and Astronomy, University of California, Irvine, CA 92697, USA

ARTICLE INFO

Available online 7 October 2014

Keywords:

Dense Kondo lattice

Extreme pressure

Fermi liquid

Electrical resistivity

Synchrotron x-ray diffraction

ABSTRACT

To investigate whether the dense Kondo compound CeB₆ might evolve into a topological insulator under sufficient pressure, four-point electrical resistivity measurements have been carried out over the temperature range 1.3 K–295 K in a diamond anvil cell to 122 GPa. The temperature T_{max} of the resistivity maximum initially increases slowly with pressure but disappears between 12 and 20 GPa. The marked changes observed under pressure suggest that a valence and/or structural transition may have occurred. Synchrotron x-ray diffraction measurements, however, fail to detect any change in crystal structure to 85 GPa. Although a transition into an insulating phase is not observed, this dense Kondo system is completely suppressed at 43 GPa, leaving behind what appears to be a conventional Fermi liquid metal.

© Elsevier B.V. All rights reserved.

1. Introduction

Many compounds and alloys containing Ce, including Ce metal, show highly anomalous magnetic properties due to the fact that the 4*f* level in trivalent Ce often lies near a magnetic instability. This led to the observation of a classic Kondo effect in the electrical resistivity measurements of Winzer [1] on the dilute magnetic alloy (La_{0.994}Ce_{0.006})B₆ to 50 mK; in these studies the Kondo temperature is estimated to lie near $T_K \rightarrow 1$ K. At higher Ce concentrations the competition between the Kondo effect and Ce–Ce exchange interactions increases, leading finally in CeB₆ to an exotic phase diagram with a prominent resistivity maximum near 4 K and two kinds of ordered phases: antiferroquadrupolar ordering below 3.2 K (phase II) and antiferromagnetic ordering below 2.3 K (phase III) [2,3]. This compound has attracted a great deal of attention following its identification as a dense Kondo system [4]. CeB₆ is metallic at ambient pressure with the simple cubic (*Pm3m*) structure [5]. The ground state of the Ce³⁺ ion is a Γ_8 quartet split by 30 K into two doublets and separated by 540 K from the excited Γ_7 doublet [6].

SmB₆ is a prime candidate for a topological Kondo insulator categorized as a heavy fermion semiconductor [7–10] with strong electron–electron correlations in which the localized 4*f* electrons give rise to novel ground states [11,12]. SmB₆ and CeB₆ both have the $J=5/2$ Hund's rule configuration [6,13]. Upon cooling below 10 K, the electrical resistivity of SmB₆ rises by orders of magnitude

as it enters into an anomalous insulating state, only to saturate near 7 m Ω cm [12]. This behavior agrees with that of a Kondo insulator where at high temperatures highly correlated electron behavior is observed, but at the lowest temperatures an insulating state emerges as a bulk band gap opens up through the hybridization of localized 4*f* states with 5*d* conduction electrons [7–10]. Since the primary effect of high pressure on a dense Kondo system is to enhance this hybridization [15], it is conceivable that sufficient pressure might succeed in transporting CeB₆ into the topological Kondo insulator regime or possibly effect a change in Ce's valence or even a volume collapse similar to that observed in pure Ce [16].

To date there have been relatively few studies of the transport and magnetic properties of CeB₆ at high pressures [15,17,18]. Kobayashi et al. [15] report that the prominent resistivity maximum in CeB₆ shifts from 3.6 K to ~ 7 K at 13 GPa pressure, but there is no evidence for a transition to a Kondo insulating state as in SmB₆ [12]. There is also no evidence for a structural phase transition in CeB₆ at ambient temperature to 20 GPa [19].

In the present study we extend the previous resistivity experiments to significantly higher pressures (122 GPa). The resistivity maximum is found to initially shift to somewhat higher temperatures with pressure, but rapidly decreases in magnitude, finally disappearing completely at 20 GPa. The present experiments fail to find any evidence that CeB₆ transforms into a Kondo insulating state to 122 GPa in the temperature range 1.3–295 K. However, pressures of 43 GPa and above are sufficient to completely suppress the anomalies associated with CeB₆'s dense Kondo state. These dramatic changes under pressure are not due to structural

* Corresponding author. Fax: +1 314 935 6239.

E-mail address: jss@wuphys.wustl.edu (J.S. Schilling).

phase transitions, as evidenced by x-ray diffraction studies at 15 K to 85 GPa. However, we cannot exclude the possibility that a pressure-induced change in Ce's valence (Ce^{3+} to Ce^{4+}) may have occurred.

2. Experimental methods

Single crystals of CeB_6 were grown in Al flux by slow cooling from 1450 °C. The crystals were removed from the Al flux by leaching in NaOH solution [20]. The lattice parameter of the resulting simple cubic crystals was measured to be 4.132(4) Å.

High pressure dc electrical resistivity measurements were carried out in a diamond-anvil cell (DAC) using two opposing 1/6-carat, type-Ia diamond anvils with 0.35 mm culets beveled at 7° to 0.18 mm central flats. A Re gasket (6–7 mm diameter, 250 μm thick) was preindented to 30 μm and insulated using a 4:1 c-BN-epoxy mixture which also served as a quasi-hydrostatic pressure medium. The pressure was determined *in situ* by placing two small ruby spheres [21] in the sample space. Four-point resistivity was measured using four leads cut from a thin Pt foil (see Fig. 1); two extra leads were connected to the Re gasket to detect any electrical shorts. A single crystal sample (dimensions 40 \times 40 \times 5 μm^3) was placed on top of the Pt leads and electrical contact was made by pressing the sample into the leads with the opposing anvil. During the course of the experiment the sample was plastically deformed by the quasi-hydrostatic pressure. To keep the power dissipated in the sample below 1 μW , an excitation current of \sim 1 mA was used. A reduction of the current to 0.1 mA at the lowest temperature (1.3 K) caused no measurable change in the sample resistance.

A He-gas driven membrane allowed changes in pressure at any temperature above 3 K. The pressure cell was placed in a continuous-flow cryostat (Oxford Instruments) and submerged in pumped liquid He to reach temperatures as low as 1.3 K. The pressure was determined either at ambient temperature (295 K) or at low temperature (5–10 K) with a resolution of \pm 0.2 GPa using the revised ruby pressure scale of Chijioke et al. [22]. Raman spectroscopy [23] on the diamond vibron was also used to

determine the pressure in the upper pressure range where the ruby fluorescence became very weak. Further details of the high pressure resistivity techniques are given elsewhere [24].

High-pressure low-temperature powder x-ray diffraction (XRD) experiments were carried out at the HPCAT (16-BM-D) beamline of the Advanced Photon Source, Argonne National Laboratory. A symmetric DAC (Princeton shops) was prepared using standard diamond anvils with 300 μm diameter culets beveled to 180 μm . The anvils were glued onto WC and B_4C seats, the latter allowing the extension of the 2θ range to \sim 25°. A Re gasket was preindented to 25 μm and a hole 90 μm in diameter laser drilled through the center of the indentation to serve as sample chamber.

Powdered CeB_6 was placed into the sample chamber together with Au powder as pressure marker and a ruby sphere. He gas was then loaded using the GSECARS/COMPRES system [25] to \sim 8.6 GPa as determined by ruby fluorescence [22]. During the high-pressure x-ray experiment the *in situ* pressure was determined from the known equation of state of Au [26].

The pressure cell was cooled using a He flow cryostat. Isothermal measurements were performed at \sim 15 K and the pressure was increased at low temperature using a gear box. Photons of 29.2 keV energy compressed the reciprocal space, thus allowing a significant number of Bragg reflections within the limited 2θ range. Diffraction was detected in angular dispersive mode using an image plate (MAR3450) with 100 \times 100 μm^2 pixel size located 324.37 mm from the sample. The beam was focused to \sim 15 \times 5 μm^2 by a pair of Kirkpatrick-Baez mirrors. The 2D diffraction patterns were converted to intensity versus 2θ using Fit2D software [27]. CeB_6 and Au diffraction patterns were concomitantly fit using Le Bail and Rietveld methods implemented with GSAS/EXPGUI software [28,29].

3. Results of experiment

3.1. Electrical resistivity measurements

In Fig. 2 is shown resistance versus temperature for the high-pressure data obtained on CeB_6 over the temperature range 1.3 K–295 K. The order of measurement is: 0.5, 7.7, 12, 20, 30, 43, 122 GPa. Above 10 K all data shown were taken with increasing temperature due to the relatively slow rate of warming to 295 K (12 h). Pressure was always applied at 295 K. All values of pressure given in Fig. 2 were measured at 295 K before cooling down; the values of the pressure after cooling to 5–10 K and after warming back up to 295 K, all at the same gas pressure in the membrane, are given in parentheses in the caption to Fig. 2, if they were measured. The highest pressure reached, 122 GPa, was determined from Raman scattering off the diamond vibron.

At 0.5 GPa the temperature-dependent resistance $R(T)$ is seen in Fig. 2 to display a minimum near 110 K followed at lower temperatures by a peak at $T_{\text{max}} \leftarrow$ 7.5 K, a higher temperature than that, $T_{\text{max}} \rightarrow$ 3.5 K, reported in earlier measurements on CeB_6 in the 0–1 GPa pressure range [15,30,31]. Kobayashi et al. [15] find that T_{max} shifts to higher temperatures with pressure, reaching \sim 7 K at 13 GPa. In the present experiment T_{max} is also observed to increase with pressure (T_{max} reaches 12.8 K at 7.7 GPa and 14.8 K at 12 GPa), the resistivity peak itself diminishing rapidly in size and finally disappearing at a pressure between 12 and 20 GPa. For pressures up to and including 30 GPa, the resistance below 100 K decreases with pressure; for temperatures above 20 K the decrease in resistance between 30 and 43 GPa is particularly large. This decrease likely reflects the intrinsic pressure dependence of the CeB_6 sample since any plastic deformation of the sample by the solid pressure medium would be expected to enhance its resistance.

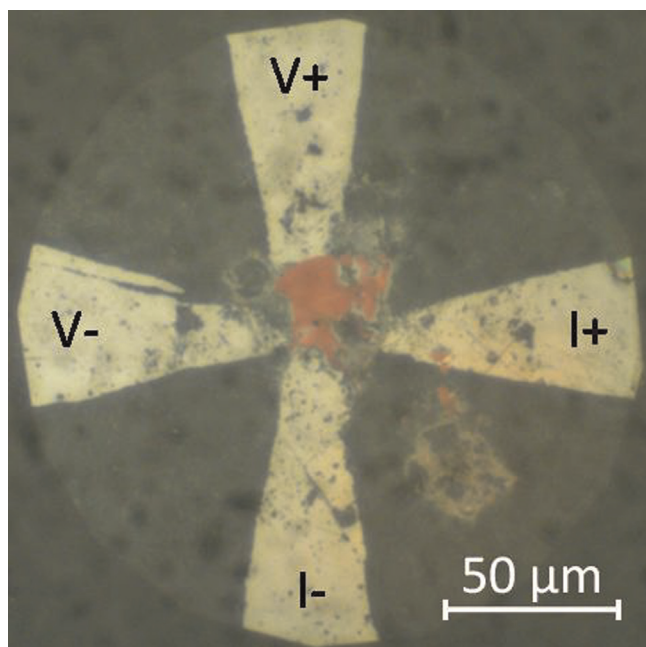


Fig. 1. Image of red CeB_6 sample (40 \times 40 \times 5 μm^3) resting on four Pt leads (4 μm thick) on insulated Re gasket. (For interpretation of the references to color in this figure caption, the reader is referred to the web version of this article.)

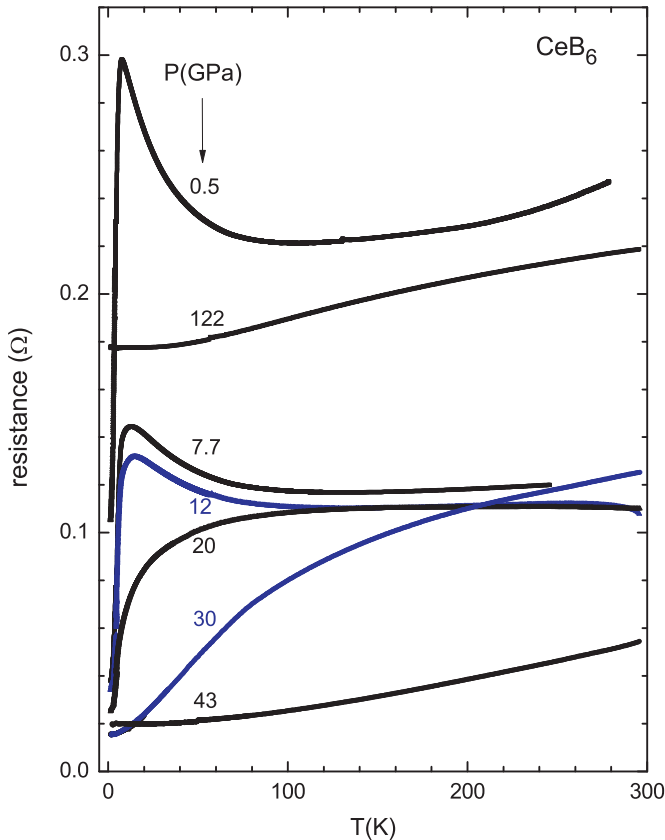


Fig. 2. Electrical resistance of CeB_6 versus temperature at pressures in GPa measured at 295 K before cooling. Numbers in parentheses after each pressure give pressures measured at 5–10 K after cooling (left) and at 295 K after warming back to 295 K (right): 0.5(1.2, 0.8), 7.7(–0.8.5), 12(–0.14), 20(24.5, –), 30(35, 31), 43 (52, 45), 122(–, 129). A dash “–” indicates the pressure was not measured.

As the pressure was increased above 43 GPa, however, the resistance at ambient temperature began to shift upwards and change with time at a given pressure, indicating relaxation behavior in the pressure cell. The two ruby spheres were also seen to move away from the sample, preventing a reliable determination of the sample pressure. At 122 GPa the pressure was determined from the diamond anvil vibron using Raman spectroscopy. In Fig. 2 it is seen that the entire resistance curve $R(T)$ at 122 GPa has risen to a significantly higher value, *nine times* that at 43 GPa. The reason for the large increase in resistance is not clear, but could be the result of a structural phase transition with a mixed phase region, leading to enhanced defect scattering. Alternatively, the outward flow of the pressure cell could generate a large number of lattice defects in the sample from plastic deformation by the solid pressure medium. In any case, to 122 GPa no sharp upturn in the electrical resistivity of CeB_6 below 10 K was observed that might have signaled a transition into a topological insulating state, as suggested for SmB_6 [12].

Following the measurement at 122 GPa, the pressure was released completely. The $R(T)$ dependence was similar to that at 122 GPa but shifted to even higher resistance values. In addition, the characteristic resistivity maximum seen near 6 K at 0.5 GPa was *not* recovered at ambient pressure. This finding would be consistent with a structural phase transition at extreme pressures that remained metastable after releasing to ambient pressure.

The dramatic changes observed in the temperature-dependent resistivity of CeB_6 under pressure from 0.5 to 43 GPa suggest that a change in valence and/or a structural transition may have taken place. Previous diffraction studies by Leger et al. [19] at ambient temperature revealed no phase transition to 20 GPa. High pressure

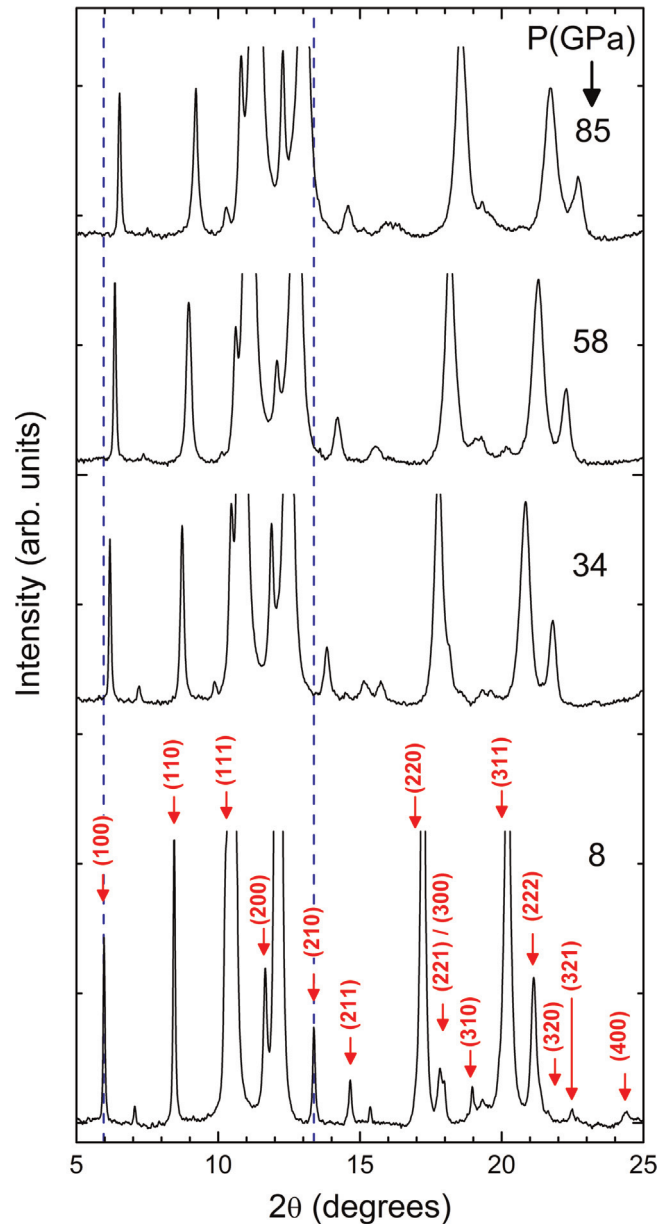


Fig. 3. CeB_6 diffraction pattern at 15 K and selected pressures. Large, truncated peaks are from Au marker. Red arrows and indices give positions of CeB_6 peaks; all other peaks can be assigned to Au, ruby or Re. (For interpretation of the references to color in this figure caption, the reader is referred to the web version of this article.)

x-ray diffraction and x-ray absorption near-edge structure (XANES) studies to pressures of at least 50 GPa would be helpful to clarify the situation. We next discuss the results of our recent x-ray diffraction measurements on CeB_6 to pressures exceeding 50 GPa.

3.2. X-ray diffraction measurements

The x-ray diffraction pattern of CeB_6 at 15 K for selected hydrostatic pressures with He pressure medium is shown in Fig. 3. Neither the emergence of new Bragg peaks, nor the splitting of existing peaks, was observed to the highest pressure (85 GPa), indicating that the structure of CeB_6 remains simple cubic throughout this range.

The pressure dependence of the unit cell volume is well described by a 3rd order Birch-Murnaghan equation of state [32]

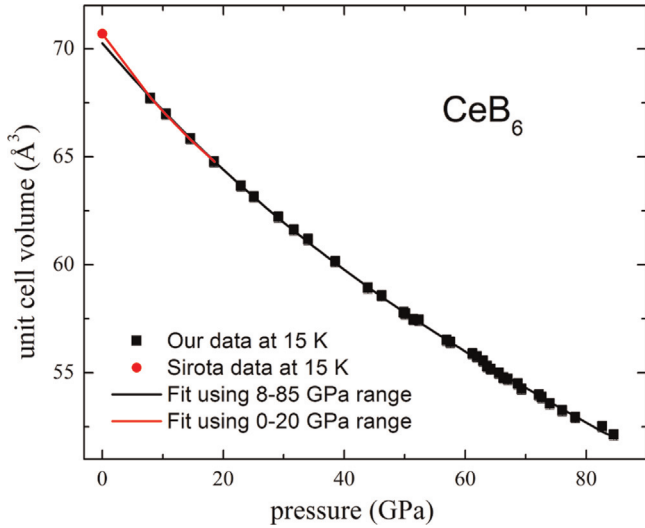


Fig. 4. Pressure dependence of unit cell volume of CeB₆ at 15 K. Error bars are smaller than symbols. Data are fit 3rd order Birch–Murnaghan equation of state [32]. Black curve fits present data 8–85 GPa. Red curve fits 4 data points 8–20 GPa plus point at 0 GPa from Sirota et al. in Ref. [33]. Fit parameters are given in Table 1. (For interpretation of the references to color in this figure caption, the reader is referred to the web version of this article.)

(see Fig. 4):

$$P(V) = \frac{3B_0}{2} \left[\left(\frac{V_0}{V} \right)^{7/3} \mathcal{B} \left(\frac{V_0}{V} \right)^{5/3} \right] - \left\{ 1 + \frac{3}{4} \left(B_{\mathcal{B}} \mathcal{B} 4 \right) \left[\left(\frac{V_0}{V} \right)^{2/3} \mathcal{B} 1 \right] \right\}, \quad (1)$$

where P and V are the measured pressure and volume, respectively. The fit to the data using Eq. (1) yields the ambient pressure volume V_0 , bulk modulus B_0 , and pressure derivative of the bulk modulus $B_{\mathcal{B}}$. The fit parameters are summarized in Table 1 together with those reported in the literature. The first fit includes only the present $V(P)$ data measured from 8 to 85 GPa. The resulting black fit curve is seen in Fig. 4 to lie slightly below the ambient pressure volume V_0 from Sirota et al. [33]. In Table 1 it can be seen that the value of V_0 lies below the literature values, whereas the bulk modulus B_0 lies above these values. Much better agreement is achieved if Eq. (1) is fit to the lowest 5 high pressure points to 20 GPa in Fig. 4, including the ambient pressure point from Sirota et al. [33]. This excellent agreement is not surprising since the literature studies were all carried out at pressures at or below 20 GPa.

Table 1
Summary of literature values of unit cell volume of CeB₆ at ambient pressure V_0 , bulk modulus B_0 , and pressure derivative of bulk modulus $B_{\mathcal{B}}$ compared to present results (see Fig. 4). “DFT” stands for “Density Functional Theory”.

Method	P (GPa)	T (K)	V_0 Å ³	B_0 (GPa)	$B_{\mathcal{B}}$	Reference
x-ray	8–85	15	70.3 (3)	204(10)	2.5	This paper
x-ray	0–20	15	70.69 (9)	167(8)	5.4	This paper
x-ray	0	15	70.7	–	–	[33]
x-ray	0–20	300	71.27	166	3.2	[19]
x-ray	0–10	300	70.86	159	–	[17]
Ultrasound	0	10	–	191	–	[36]
Ultrasound	0	300	–	168	–	[37]
Brillouin scattering	0	300	–	182	–	[37]
DFT	0	300	72.47	173	3.9	[38]
DFT	0	0	71.16	162	–	[39]

Although no structural phase transition was detected to 85 GPa pressure, one cannot exclude the possibility of a change in structure in the region 85–122 GPa that led to the strong increase in $R(T)$ at 122 GPa.

4. Discussion

Pressures exceeding 43 GPa cause drastic changes in the temperature-dependent resistance $R(T)$ of CeB₆ that indicate a complete suppression of its dense Kondo state. The prominent resistivity peak near ambient pressure disappears between 12 and 20 GPa and $R(T)$ is strongly suppressed over nearly the entire measured temperature range as the pressure is increased to 43 GPa.

It is well known that in Ce systems exhibiting Kondo effect phenomena, the Kondo temperature T_K increases rapidly with pressure [34]. In the dilute magnetic alloy (La_{0.994}Ce_{0.006})B₆ the electrical resistivity decreases with increasing temperature from its giant unitarity limit value and passes through a minimum near $T_{\min} \rightarrow 20$ K before rising rapidly as the phonons of the stiff LaB₆ host lattice become thermally excited; the Kondo temperature in this dilute magnetic alloy is estimated to lie near 1 K [1]. The increase in T_K with pressure comes from the increasing hybridization between the 4*f* and conduction electrons that enhances the negative covalent mixing exchange interaction responsible for the Kondo phenomena. As T_K increases with pressure, the temperature of the resistivity minimum T_{\min} in a dilute Kondo system would be expected to first slowly increase with pressure, but then begin to decrease after T_K becomes larger than T_{\min} [34].

In the dense Kondo compound CeB₆, T_{\min} lies near 110 K at both ambient [30,31] and 0.5 GPa pressure (see Fig. 2). The higher value of T_{\min} for CeB₆ (110 K) compared to that for the dilute magnetic alloy (20 K) is due to the much higher Ce concentration in the former. The marked resistivity maximum in CeB₆ arises from magnetic Ce–Ce interactions and coherence effects in the Kondo lattice. Due to the increase of its Kondo temperature with pressure, T_{\min} for CeB₆ increases with pressure from 0.5 GPa to 7.7 GPa to 12 GPa, disappearing completely at 20 GPa and above. However, it is difficult to understand why the resistivity of CeB₆ does not increase over the measured temperature range as the Kondo temperature moves to ever higher temperatures, as would be expected for a dilute magnetic Kondo alloy [34].

The unexpected overall rapid decrease in $R(T)$ for CeB₆ as the pressure increases to 43 GPa could be taken to suggest that a valence transition occurs in the Ce cation. A pressure-induced change of Ce’s valence from Ce³⁺ to Ce⁴⁺ would leave the Ce cation devoid of 4*f* electrons and, therefore, completely quench the dense Kondo state, whereby $R(T)$ would decrease significantly. At 43 GPa the temperature dependence of the resistivity looks much like that of a conventional Fermi liquid metal. Unfortunately, the signal/noise ratio in this experiment is not sufficient to establish whether or not the relation $\rho(T) \propto T^2$ holds, as one would expect from a Fermi liquid at sufficiently low temperatures.

The valence-change scenario receives some support from the fact that the temperature-dependent part of the resistivity at 43 GPa can be estimated [35] to change by only $\kappa R \rightarrow 9$ tΩ cm from 295 K to 1.3 K. This value of κR is well below than that found for pure La [40], which contains no 4*f* electrons, and is only about six times greater than that for pure copper, one of the best conductors known. It would be of considerable interest to carry out XANES measurements on CeB₆ to pressures of at least 50 GPa to establish whether or not Ce in CeB₆ undergoes a valence change from Ce³⁺ to Ce⁴⁺.

In summary, electrical resistivity measurements on CeB₆ from 1.3 K to 295 K to pressures as high as 122 GPa fail to find any

evidence for a transition into a topological insulating state. However, pressures of 43 GPa are found to completely transform CeB₆ from a dense Kondo system into what appears to be an ordinary Fermi liquid metal. Future high-pressure synchrotron spectroscopy studies are recommended to shed light on the exact nature of this transformation and to establish whether or not it is driven by an increase in valence.

Acknowledgments

The authors would like to express gratitude to T. Matsuoka and K. Shimizu for sharing information on their high-pressure electrical resistivity techniques used in this study. Thanks are due A. Gangopadhyay for his critical reading of the manuscript. This work was supported by the National Science Foundation (NSF) through Grant No. DMR-1104742 and by the Carnegie/DOE Alliance Center (CDAC) through NNSA/DOE Grant No. DE-FC52-08NA28554. Work at Argonne National Laboratory is supported by the U.S. Department of Energy, Office of Science, under contract No. DE-AC02-06CH11357.

References

- [1] K. Winzer, *Solid State Commun.* 16 (1975) 521.
- [2] K. Winzer, W. Felsh, *J. Phys. (Paris)* 39 (1978) C6–832.
- [3] R. Shiina, H. Shiba, P. Thalmeier, *J. Phys. Soc. Jpn.* 66 (1997) 1741.
- [4] T. Kasuza, K. Takegahara, Z. Aoki, K. Hanyawa, M. Kasaza, S. Kunii, T. Fujita, N. Sato, H. Kimura, T. Komatsubara, T. Furuno, J. Rossat-Mignod, in: L. M. Falicov, W. Hanke, M.B. Maple (Eds.), *Valence Fluctuations in Solids*, North-Holland, Amsterdam, 1981, p. 215.
- [5] J.M. Leger, *Revue Phys. Appl.* 19 (1984) 815.
- [6] E. Zirngiebl, B. Hillebrands, S. Blumenröder, G. Güntherodt, M. Löwenhaupt, J. M. Carpenter, K. Winzer, Z. Fisk, *Phys. Rev. B* 30 (1984) 4052.
- [7] G. Aeppli, Z. Fisk, *Comm. Condens. Matter Phys.* 16 (1992) 155.
- [8] P. Riseborough, *Adv. Phys.* 49 (2000) 257.
- [9] P.W. Anderson, *Phys. Rev. Lett.* 104 (2010) 176403.
- [10] P. Coleman, in: *Handbook of Magnetism and Advanced Magnetic Materials*, vol. 1, Wiley, 2007, pp. 95–148.
- [11] J. Jiang, S. Li, T. Zhang, Z. Sun, F. Chen, Z.R. Ye, M. Xu, Q.Q. Ge, S.Y. Tan, X.H. Niu, M. Xia, B.P. Xie, Y.F. Li, X.H. Chen, H.H. Wen, D.L. Feng, *Nat. Commun.* 4 (2013) 3010.
- [12] M. Neupane, N. Alidoust, S.-Y. Xu, T. Kondo, Y. Ishida, D.J. Kim, C. Liu, I. Belopolski, Y.J. Jo, T.-R. Chang, H.-T. Jeng, T. Durakiewicz, L. Balicas, H. Lin, A. Bansil, S. Shin, Z. Fisk, M.Z. Hasan, *Nat. Commun.* 4 (2013) 2991.
- [13] P. Nyhus, S.L. Cooper, Z. Fisk, J. Sarrao, *Phys. Rev. B* 55 (1997) 12488; P.A. Alekseev, V.N. Lazukov, R. Osborn, B.D. Rainford, I.P. Sadikov, E. S. Konovalova, Yu.B. Paderno, *Europhys. Lett.* 23 (1993) 347.
- [15] T.C. Kobayashi, K. Hashimoto, S. Eda, K. Shimizu, K. Amaya, Y. Onuki, *Phys. B* 281–282 (2000) 553.
- [16] See, for example: J.W. Allen, R.M. Martin, *Phys. Rev. Lett.* 49 (1982) 1106, and references therein.
- [17] N.B. Brandt, V.V. Moshchalkov, S.N. Pashkevich, M.G. Vybornov, M.V. Semenov, *Solid State Commun.* 56 (1985) 937.
- [18] M. Takashita, H. Aoki, C.J. Haworth, T. Terashima, S. Uji, C. Terakura, T. Matsuomoto, A. Uesawa, T. Suzuki, R. Settai, Y. Onuki, N. Sato, S. Kunii, T. Nishigaki, H. Sugawara, Y. Aoki, H. Sato, *Rev. High Pressure Sci. Technol.* 7 (1998) 456.
- [19] J.M. Leger, J. Rossat-Mignod, S. Kunii, T. Kasuya, *Solid State Commun.* 54 (1985) 995.
- [20] P.C. Canfield, Z. Fisk, *Phil. Mag.* B 65 (1992) 1117.
- [21] J.C. Chervin, B. Canny, M. Mancinelli, *High Pressure Res.* 21 (2001) 305.
- [22] A.D. Chijioke, W.J. Nellis, A. Soldatov, I.F. Silvera, *J. Appl. Phys.* 98 (2005) 114905.
- [23] Y. Akahama, H. Kawamura, *J. Appl. Phys.* 100 (2006) 043516.
- [24] K. Shimizu, K. Amaya, N. Suzuki, *J. Phys. Soc. Jpn.* 74 (2005) 1345.
- [25] M. Rivers, V.B. Prakapenka, A. Kubo, C. Pullins, C.M. Holl, S.D. Jacobsen, *High Press. Res.* 28 (2008) 273.
- [26] W.B. Holzapfel, M. Hartwig, W. Sievers, *J. Phys. Chem. Ref. Data* 30 (2001) 515.
- [27] A.P. Hammersley, S.O. Svensson, M. Hanfland, A.N. Fitch, D. Häusermann, *High Press. Res.* 14 (1996) 235.
- [28] A.C. Larson, R.B. Von Dreele, Los Alamos National Laboratory Report LAUR, 86-748, 1994.
- [29] B.H. Toby, *J. Appl. Cryst.* 34 (2001) 210.
- [30] N.E. Sluchanko, A.V. Bogach, V.V. Glushkov, S.V. Demishev, V.Yu. Ivanov, M. I. Ignatov, A.V. Kuznetsov, N.A. Samarin, A.V. Semeno, N.Yu. Shitsevalova, *J. Exper. Theor. Phys.* 104 (2007) 120.
- [31] N. Mōri, N. Sato, T. Kasuya, in: S. Minomura (Ed.), *Solid State Physics under Pressure: Recent Advance with Anvil Devices*, Springer-Verlag, NY, 1985, p. 259.
- [32] F. Birch, *Phys. Rev.* 71 (1947) 809.
- [33] N.N. Sirota, V.V. Novikov, A.V. Novikov, *Phys. Sol. State* 42 (2000) 2093.
- [34] See, for example: J.S. Schilling, *Adv. Phys.* 28 (1979) 657.
- [35] From Ref. [31] the value of the resistivity at T_{\min} at ambient pressure is $\sim 78 \mu\Omega \text{ cm}$, thus allowing us to calibrate the resistance values in Fig. 2.
- [36] S. Nakamura, T. Goto, S. Kunii, K. Iwashita, A. Takami, *J. Phys. Soc. Jpn.* 63 (1994) 623.
- [37] B. Lüthi, S. Blumenröder, B. Hillebrands, E. Zirngiebl, G. Güntherodt, K. Winzer, *Z. Phys. B* 58 (1984) 31.
- [38] T. Gürel, R. Eryiğit, *Phys. Rev. B* 82 (2010) 104302.
- [39] Sandeep, M.P. Ghimire, D.P. Rai, P.K. Patra, A.K. Mohanty, R.K. Thapa, *J. Phys.: Conf. Ser.* 377 (2012) 012084.
- [40] N.R. James, S. Legvold, F.H. Spedding, *Phys. Rev.* 88 (1952) 1092.